

Pure phase encode magnetic field gradient monitor

Hui Han, Rodney P. MacGregor, Bruce J. Balcom*

MRI Centre, Department of Physics, University of New Brunswick, Fredericton, New Brunswick, Canada E3B 5A3

ARTICLE INFO

Article history:

Received 2 April 2009

Revised 15 September 2009

Available online 17 September 2009

Keywords:

NMR probe

Micro RF coil

Pure phase encode

Gradient waveform

Eddy current

k -space trajectory

Magnetic field monitoring (MFM)

ABSTRACT

Numerous methods have been developed to measure MRI gradient waveforms and k -space trajectories. The most promising new strategy appears to be magnetic field monitoring with RF microprobes. Multiple RF microprobes may record the magnetic field evolution associated with a wide variety of imaging pulse sequences. The method involves exciting one or more test samples and measuring the time evolution of magnetization through the FIDs. Two critical problems remain. The gradient waveform duration is limited by the sample T_2^* , while the k -space maxima are limited by gradient dephasing.

The method presented is based on pure phase encode FIDs and solves the above two problems in addition to permitting high strength gradient measurement. A small doped water phantom (1–3 mm droplet, $T_1, T_2, T_2^* < 100 \mu\text{s}$) within a microprobe is excited by a series of closely spaced broadband RF pulses each followed by FID single point acquisition. Two trial gradient waveforms have been chosen to illustrate the technique, neither of which could be measured by the conventional RF microprobe measurement. The first is an extended duration gradient waveform while the other illustrates the new method's ability to measure gradient waveforms with large net area and/or high amplitude. The new method is a point monitor with simple implementation and low cost hardware requirements.

© 2009 Elsevier Inc. All rights reserved.

1. Introduction

Linear magnetic field gradients play a central role in MR imaging. Their functions include encoding spatial information and sensitizing the image contrast to coherent or incoherent motion. Fast, efficient MRI measurements rely on magnetic field gradient waveforms with high temporal fidelity.

Rapid switching of the magnetic field gradients leads to rapidly changing magnetic flux through the RF coil, RF shield, main magnet components and other structures. This changing magnetic flux leads to eddy currents being induced in conducting pathways near the magnet bore. Hardware improvements such as shielded gradient coils and waveform pre-emphasis are largely successful at reducing these effects in modern scanners. Residual eddy currents may however still cause image-quality problems [1] including ghosting in EPI, RARE and GRASE imaging pulse sequences [2], slice-profile modulation with spatial-spectral RF pulses [3], geometric distortion in diffusion-weighted EPI [4], and quantitative velocity errors in phase-contrast imaging [5]. Knowledge of the true gradient waveform in the MRI pulse sequence is critical to addressing and remedying such problems.

Numerous methods have been developed to measure MRI gradient waveforms and k -space trajectories [6–14]. The most promising new strategy appears to be magnetic field monitoring (MFM) with RF microprobes [15,16]. In this method multiple RF

microprobes record the magnetic field evolution associated with a wide variety of imaging pulse sequences.

The MFM method involves exciting the sample and measuring the time evolution of magnetization through the FID. The gradient waveform duration is limited by the sample T_2^* . The k -space maxima (i.e. maximum temporal gradient area or image resolution) measurable with MFM are limited by gradient dephasing. In addition, implementation of this technique is relatively complex. It requires careful probe fabrication, an array of at least 3 probes, accurate probe positioning and alignment and a multi channel receiver.

The new method presented is a pure phase encode version of the MFM measurement for mapping magnetic field gradient waveforms. A heavily doped small water droplet (diameter ≤ 1 –3 mm) within a micro RF coil is excited by a series of closely spaced broadband RF pulses each followed by FID single point acquisition. Based on pure phase encoding, the method naturally has no limitation on k -space extrema with correspondingly high image resolution and maximum gradient area. Neither does it have a limitation for long duration gradient waveforms/ k -space trajectories.

Two trial gradient waveforms have been chosen to illustrate the advantages of the technique. Neither could be measured by conventional MFM. One illustrates the ability to measure extended duration magnetic field gradient waveforms while the other illustrates the ability to measure magnetic field gradient waveforms with large net gradient area and/or high amplitude (a simple bipolar diffusion gradient waveform, $G_{\text{max}} = 250 \text{ mT/m}$, b value approx = $100,000 \text{ s/mm}^2$).

* Corresponding author. Fax: +1 506 453 4581.

E-mail address: bjb@unb.ca (B.J. Balcom).

For most diffusion imaging sequences (e.g., diffusion-weighted EPI), the diffusion sensitization b value is on the order of 1000 s/mm². The diffusion sensitizing gradients employed are usually the maximal gradient strength which can be provided by the MRI scanner. However, large gradient switching will induce eddy currents even in MRI systems with good eddy current compensation. The eddy currents may cause various artifacts (e.g., geometric distortion) in diffusion-weighted images [23,24]. It is desirable to measure the diffusion gradient waveforms associated with the diffusion-weighted imaging sequence for post acquisition image processing or pre-adjusting the gradient waveform to eliminate the eddy current effects.

The RF micro coil utilized is extremely easy to fabricate, compared with MFM RF microprobes [15,16]. Susceptibility matching for improved static field homogeneity is not an issue. One small probe is sufficient to measure all three gradient axes and a multi channel receiver is not a prerequisite. The method is a point monitor where the probe location does not need be exactly known.

The RF micro coil utilized provides a high measurement sensitivity compared with our previous work [17] due to the maximized probe filling factor and a stronger B_1 field per unit current [18,19]. Our previous study, employed a thin uniform cylindrical gel sample. It is however hard to make a thin slice phantom (thickness <3 mm) and position it orthogonal to 3 gradient directions sequentially. The new method does not require phantom movement for 3 dimensional gradient measurements.

2. Theory

2.1. Small NMR probe for gradient monitor

For magnetic field gradient measurements, transverse magnetization dephasing due to the gradient is always an issue. Smaller samples are usually required to limit signal decay due to gradient dephasing. This naturally suggests a correspondingly small RF probe. The proposed method acquires a FID single point after a short phase encoding time t_p following each RF excitation. Therefore it has a significant advantage against gradient dephasing compared with conventional MFM. Although a true microcoil [21] will work efficiently with this strategy, a small NMR coil (phantom size from mm to a few cm) with simple fabrication is generally suitable.

2.2. Pure phase encode

The waveform measurement pulse sequence is illustrated in Fig. 1. A series of broadband RF pulses are employed to create transverse magnetization in the presence of the gradient. A sample

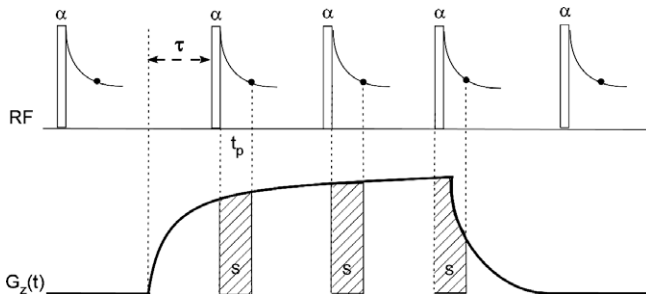


Fig. 1. Pulse sequence employed to measure the gradient waveform. A series of low flip angle RF pulses are applied in each execution of the pulse sequence. RF pulses prior to the gradient pulse provide a reference phase. Following each RF excitation a single FID point is acquired after a phase encoding time t_p . The phase is measured to determine gradient area S and thereby the gradient amplitude at a specific time. Repeating the basic measurement while incrementing τ yields a high temporal resolution in the final measurement.

with very short T_1 , T_2 ensures each RF excitation is independent of all other excitations i.e. the sample magnetization will be at equilibrium for each pulse. Following each RF excitation after a fixed duration, t_p , the FID single point is acquired. With each repetition of this basic measurement sequence, following necessary signal averaging, the time variable τ is incremented. The gradient waveform can thus be measured with high temporal resolution.

With a spherical sample displaced along the axis of magnetic field gradient G_z , with an offset z_0 relative to the gradient origin, the FID single point phase [17] is

$$\theta = \gamma G_z t_p z_0. \quad (1)$$

The FID single point phase is thus a direct measurement of average gradient amplitude G_z during the chosen measurement interval t_p .

The analytical 1D Fourier Transformation of a sphere gives the magnitude of the FID single point:

$$|S(k)| = 2\pi a^3 \text{Sinc}(2\pi ka) + \left(\frac{1}{2\pi^2 k^3} - \frac{a^2}{k} \right) \text{Sin}(2\pi ka) - \frac{a}{\pi k^2} \text{Cos}(2\pi ka), \quad (2)$$

where k is $\gamma/2\pi G_z t_p$ and a is the radius of the sphere. Eq. (2) is a Sinc like function with the first zero crossing at $k = 0.72/a$. The finite size of the sample will yield a range of precession frequencies, which leads to a spread in phase of the sample. The overall phase shift is governed by Eq. (1). The signal amplitude is governed by Eq. (2).

For conventional MFM based on frequency encoding, the highest k is limited by Eq. (2). For a sphere, k must be smaller than $0.72/a$ to avoid gradient dephasing. Spatial resolution in a common 2D Cartesian k -space image is thus limited to $a/1.01$ [16]. High k -space values correspond to large net gradient areas by definition, $k = \frac{\gamma}{2\pi} \int_0^t G(t') dt'$. For the new method with pure phase encoding, the gradient waveform is measured by decomposing the large gradient area into small separate gradient areas with a short duration t_p . Thus for the same sample geometry, the new method can readily measure two orders of magnitude higher k -space compared to conventional MFM. For the same reason the new method can measure gradient amplitudes more than two orders of magnitude greater than for MFM.

Note that G_z is the average gradient amplitude during the chosen measurement interval t_p . If we choose an encoding time which is sufficiently short, then it is reasonable to assume that the gradient amplitude changes linearly during the encoding time [17]. This allows us to use the average gradient amplitude to represent the gradient amplitude at the midpoint of the interval t_p .

For extremely rapid fluctuations of gradients, with the time scale less than the minimum encoding time t_p , the measured waveform will have an artificial broadening/smoothing effect due to the averaging of gradient amplitude during the t_p interval.

3. Results and discussion

3.1. Small NMR probe and nature of the sample

Conventional MFM [15,16] involves exciting the test sample and measuring the time evolution of magnetization through the FID. The duration of the gradient waveform is thus limited by the sample T_2^* (i.e. static field inhomogeneity). The limit can be alleviated by fabricating a complex probe with susceptibility matched materials. The pure phase encode method measures the gradient waveform through measuring discrete gradient areas. One deliberately chooses a sample with a short T_2 (100 μ s). The sample T_2^* is dominated by the short T_2 and thus the probe fabrication is simple and does not require susceptibility matching.

For the pure phase encode gradient monitor, the probe does not have to be micro scale. A larger NMR coil (phantom size from mm up to a few cm) with simple fabrication is adequate for measuring a wide range of gradient amplitudes. We employ a single turn solenoidal coil [20], Fig. 2.

The small size of the test sample and associated RF probe permit the gradient waveform and non-ideal behavior, to be spatially resolved inside the MRI sample space, which is inside the MRI RF probe, by simple translation of the point sensor. There is an additional benefit associated with the small RF probe point sensor approach: The gradient waveform measurement should be undertaken in the presence of the MRI RF probe since in many instances the MRI RF probe will support eddy currents [25]. Our original approach [17] employed the MRI RF probe for the waveform measurement but this method is vulnerable to background short T_2^* signals from the probe body. The pure phase approach with a dedicated small RF probe avoids the background signal problem since it is relatively easy to eliminate all short T_2^* signal components from the home built probe.

3.2. The conical SPRITE gradient waveform measurement

Conical SPRITE [22] is a 3D, pure phase encode, Single Point Ramped Imaging with T_1 -Enhancement (SPRITE) MRI method for studies of short relaxation time systems. Conical SPRITE samples k -space with a system of modified Archimedean spiral trajectories mapped to conical surfaces.

Figs. 3 and 4 shows the 3D gradient waveforms of a single interleaved conical SPRITE k -space trajectory. The x and y gradients vary sinusoidally, while the z gradient is a stepped linear ramp. The trajectory in conical SPRITE is different from that used in frequency encoding MRI. The gradient amplitudes of each step are calculated to ensure the acquired k -space data points fall on Cartesian grid points.

The gradient waveform duration in conical SPRITE varies from hundreds of milliseconds to seconds. With conventional MFM [15,16], the transverse magnetization will completely dephase during such waveforms due to the inherent T_2^* decay. The phase will become uncertain due to a low SNR, thus a long duration gradient waveform is not measurable. However, for the pure phase encode measurement, the duration of the gradient waveform can be arbitrarily long.



Fig. 2. Photo of the single turn solenoid coil employed. A heavily $GdCl_3$ doped water drop (T_2^* , T_2 , T_1 s = 60–100 μ s) was syringed into the bulb shown at right and flame sealed. The probe was tuned to 100 MHz and capacitively matched with a Q value of 100. The probe was enclosed in an RF shield for measurement. The probe is constructed from teflon and copper and has negligible background signal.

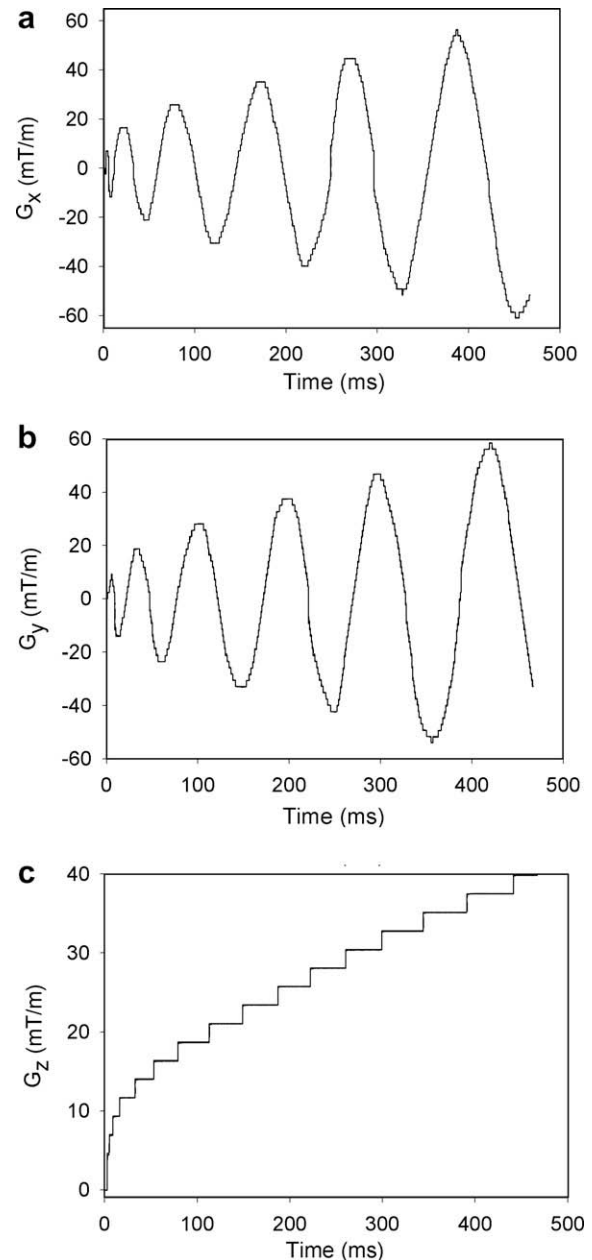


Fig. 3. Measured magnetic field gradient waveforms associated with a single conical SPRITE trajectory. The x and y gradients vary sinusoidally, while the z gradient is a stepped linear ramp. The trajectory in conical SPRITE is different from that used in frequency encoding MRI. Note in particular the discrete nature of the waveform. Ideal input waveforms (—) and measured output waveforms (---) for G_x (a), G_y (b), and G_z (c), respectively. The measured and ideal waveforms are near identical in these figures. The time resolution of the measurement is 10 μ s with 47.6 k experimental data points displayed. The waveform duration was 476 ms.

Three axis gradient waveforms, Figs. 3 and 4, were measured with the probe head positioned at approximate x , y , z offsets of 20 mm, 18 mm, 30 mm from the gradient isocenter. Fig. 3 shows the measured waveforms plotted simultaneously with the input waveforms. The y direction gradient has a slower rise time compared with the x direction gradient. There are appreciable mismatches of some gradient steps between the measured and the ideal y direction waveforms which will cause k -space misregistration in image reconstruction.

With a spherical phantom, diameter in the range 1 mm to 1 cm, with an encoding time t_p of 12.5 μ s, the method can measure gradient strengths up to 3000 mT/m and 300 mT/m respectively.

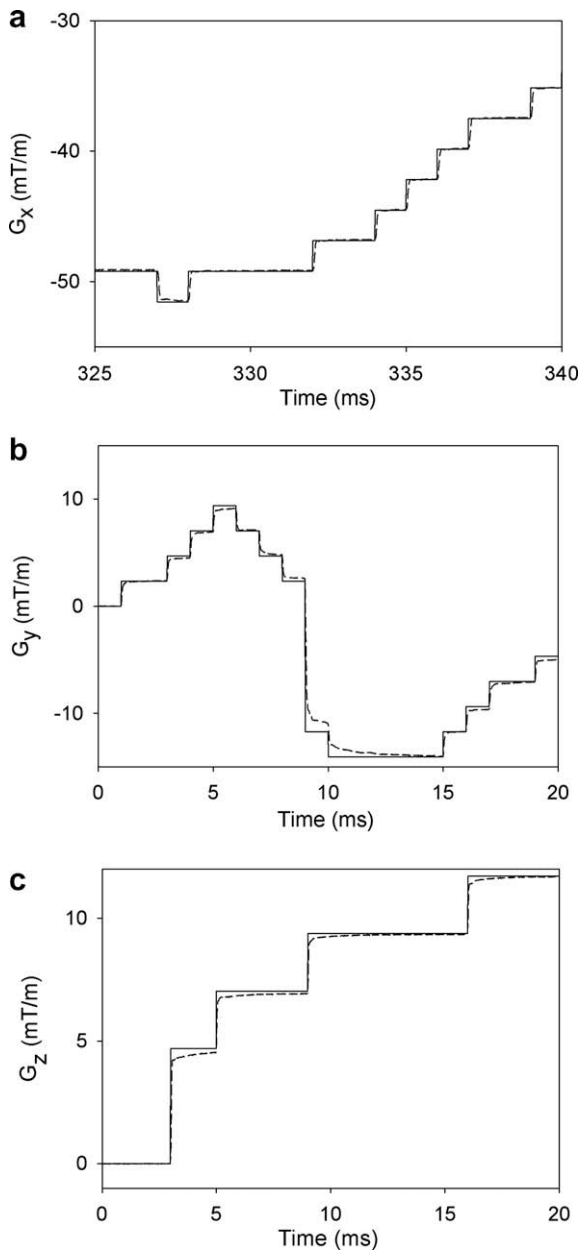


Fig. 4. Expanded portions of the gradient waveforms of Fig. 3. Ideal input waveforms (—) and measured output waveforms (---) for G_x , G_y , and G_z , respectively. Gradient G_x , (a) matches the ideal waveform quite well in the time window 325–340 ms. Gradient G_y , (b) is significantly in error in the time window 0–20 ms. The G_z gradient, (c) deviates from the ideal in the vicinity of large gradient changes in the time window 0–20 ms. The waveform temporal resolution was 10 μ s per point with 1.5 k data points displayed for x, and 2.0 k data points for y and z, respectively.

These gradient strengths cover all clinical and most non-clinical applications. Phantom sizes below 1 mm permit gradient amplitudes above 3000 mT/m to be measured.

The phantom size introduces a limit on the gradient strength maxima. However, there is no limit to the k -space extrema as long as the maximal strength of the gradient waveform associated with the imaging sequence is measurable.

3.3. Diffusion gradient waveform measurement

For conventional MFM [15,16], the net gradient area (i.e. the k value) that can be measured is limited by gradient dephasing.

For example, a sphere sample with diameter 1 mm has the maximum k value limited to 1.44 mm^{-1} and the net gradient area is limited to 34 ms mT/m. However, the net gradient area in a diffusion waveform is usually on the order of 1000 ms mT/m. Net gradient areas larger than 1000 ms mT/m occur frequently in restricted diffusion MRI measurements.

The new pure phase encode method can readily measure the gradient waveforms associated with these applications. To illustrate this advantage, a bipolar diffusion gradient waveform (b value approximately = 100,000 s/mm^2 , $G_{\text{max}} = 250 \text{ mT/m}$) was measured by the proposed method. Two trapezoidal gradient lobes with a width of 20.25 ms were separated by 40.5 ms. The trapezoidal gradient ramp time was 250 μ s. The gradient ramp time is insignificant compared to the natural rise time of the gradient and the trapezoidal gradient shape is not apparent in Fig. 5. The maximal gradient area is as large as 10,000 ms mT/m.

The simplicity of the diffusion gradient waveform permits ready analysis of the baseline and peak gradient measurement phases. The mean/standard deviation of the measured FID single point phase for a baseline measurement of 20 experimental time points, was $0^\circ/0.067^\circ$ with 64 averages and $0^\circ/0.312^\circ$ without averaging respectively. The mean baseline phase was set to zero in plotting the waveform. The mean/standard deviation of the measured FID single point phase during the gradient lobe ($G = 250 \text{ mT/m}$), 20 experimental time points, was $930.542^\circ/0.097^\circ$ with 64 averages and $930.522^\circ/0.439^\circ$ without averaging. Phases larger than 360° require unwrapping during data processing. The measured FID

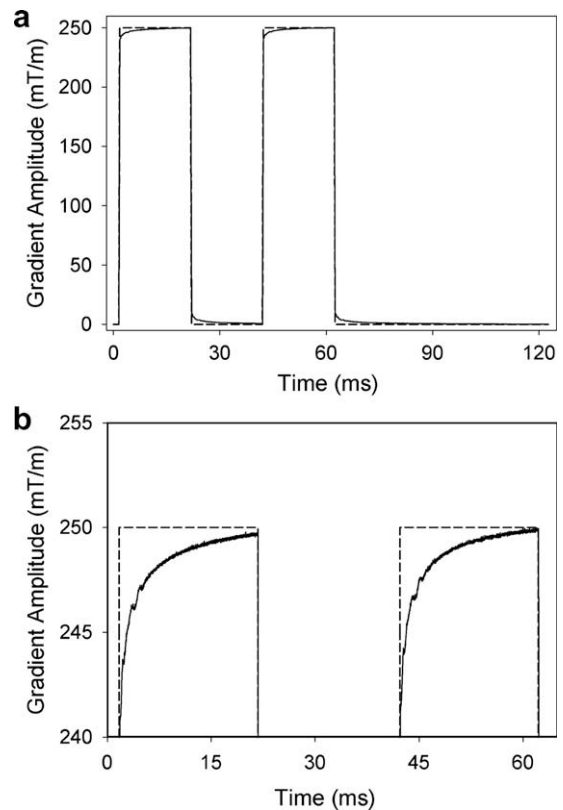


Fig. 5. (a) Bipolar diffusion gradient waveform measurement with a b value of approximately 100,000 s/mm^2 for a G_{max} of 250 mT/m. Measured gradient waveform (—) and ideal waveform (---). The maximal net gradient area is as large as 10,000 ms mT/m. (b) An expanded portion of the gradient waveform of (a) in the time window 0–60 ms. Note the maximum amplitude of the second lobe is slightly larger than the first lobe. The eddy current induced by the first gradient pulse switching contributes to the second gradient lobe. Note the measured and ideal waveforms are essentially overlapped during gradient turnover in (b). The experimental waveform resolution is 10 μ s per point.

single point magnitude during the maximum gradient ($G = 250$ mT/m), decayed to 70% of the magnitude of the analogous baseline measurement.

There was a significant difference between the ideal and the measured gradient waveforms. Note the discrepancies during the stabilization stage and during gradient turnoff.

Fig. 5(b) shows the amplitude of the second lobe is slightly larger than that of the first lobe. As anticipated, the eddy current induced by the first gradient pulse contributes to the second gradient lobe. The realistic diffusion waveform of Fig. 5 has mismatched gradient areas which differs by 0.2% as calculated from the experiment of Fig. 5. This is equivalent to a spoiling gradient of 10 ms mT/m applied after the refocusing pulse and will cause a signal attenuation larger than ideal. This would be sufficient to yield an incorrect diffusion measurement. The subtle oscillations following each gradient switch in Fig. 5(b) are caused by poor compensation of the amplifier at short time constants.

Since the entire diffusion sensitizing gradient waveform associated with an imaging pulse sequence is measured by this method, different strategies might be envisioned to compensate for the non-ideal gradient behavior/eddy current effect. One obvious strategy is to adjust the gradient waveform, guided by the waveform measurement, to better approximate ideal behavior.

4. Conclusion

A novel pure phase encode based magnetic field gradient monitor for measuring magnetic field gradient waveforms is presented. Compared with frequency encode magnetic field monitoring (MFM) with NMR microprobes, pure phase encode detection with RF microprobes has distinct advantages. (i) There is no T_2^* decay limitation on the waveform measurement and thus measurements of long duration gradient waveforms are possible; (ii) Gradient dephasing is largely alleviated by decomposing the large gradient area into small separate gradient areas with short time interval t_p and thus there is no limit on the k -space maxima or net gradient area maxima. (iii) It allows measurement of high amplitude gradients (3000 mT/m) for imaging and diffusion. (iv) Simple probe construction is possible since susceptibility matching probe components are not required.

Two gradient waveforms have been chosen to illustrate the technique that could not be measured by conventional MFM. One illustrates the ability to measure extended duration gradient waveforms while the other illustrates the ability to measure the gradient waveforms with large net gradient area or high amplitude (a simple bipolar diffusion gradient waveform, $G_{\max} = 250$ mT/m, b value approx = 100,000 s/mm²).

The presented method is a point monitor with simple implementation, low cost hardware requirement but it provides a sensitive gradient calibration tool.

It is possible to extend the method such that an array of probes and phantoms surround the sample space and the waveform measurement can be undertaken with a real sample present. This would permit the measurement of gradient cross terms and speed up the overall acquisition. Note however that such measurements will report on the gradient waveform around the sample space, not in the sample space. While real time measurements are possible with improved SNR, on balance we feel the greatest value of the method will result from gradient calibration measurements, with one or more probes, undertaken prior to scanning real samples.

5. Experimental

A spherical bulb micro cell of 3 mm inside diameter and 5 mm outside diameter was employed as the phantom (Wilma Glass,

Buena, NJ). A heavily $GdCl_3$ doped water solution (T_2^* , T_2 , $T_1 = 60$ – 100 μ s) was carefully syringed into the bulb and the bulb flame sealed.

A single turn solenoidal coil was fabricated by soldering a slotted copper tube (6 mm in OD, 4 mm in length) with a piece of rigid coaxial cable (6.35 mm in O.D, 33 cm in length) with a Teflon dielectric. The probe and sample are usually wrapped in a copper RF shield. The probe was tuned to 100 MHz and capacitively matched to 50 Ω . The probe Q value was 100. The RF amplifier output power was 10 W for a 90° pulse length of 5 μ s with a deadtime of 12 μ s. The minimum phase encode time was thus 12.5 μ s. This could be further reduced by decreasing the Q .

Gradient waveform measurements were undertaken on a Nalorac (Martinex, CA) 2.4 T 32 cm i.d horizontal bore superconducting magnet. The console was a Tecmag (Houston, TX) Apollo. A water cooled 7.5 cm i.d. gradient set was employed for gradient waveform measurements. The gradient set was driven by a Techtron (Elkhart, IN) 8710 amplifier. The RF probe was driven by a 2 kW AMT (Brea, CA) 3445 RF amplifier after 23 db attenuation.

20 RF pulses were applied prior to the gradient waveform to obtain an experimental baseline phase. Non-zero phases from instrumental effects will be corrected by the baseline measurement. The phantom location can be measured using one-dimensional SPRITE images. Since phase is proportional to the gradient amplitude, the sample location (offset to gradient origin) does not need to be exactly known. One plots the gradient waveform by scaling the measured phases to the phase of a known time invariant gradient with measured phase [17].

For each waveform gradient measurement, the time interval between consecutive RF pulses was 250 μ s. The RF pulse duration was 1 μ s for a flip angle of 18°. The experimental waveform temporal resolution was 10 μ s/point with 25 interleaved acquisitions for both the diffusion and the conical SPRITE waveforms measurements. The phase encoding time was 22 μ s with 64 averages collected for a total scan time of 5 min for the diffusion waveform measurement. The phase encoding time was 40 μ s with 64 averages collected for 15 min for each Cartesian direction of the conical SPRITE waveform measurement.

Acknowledgment

B.J.B. thanks NSERC of Canada for a Discovery grant. B.J.B. also thanks the Canada Chairs program for a Research Chair in MRI of Materials (2009–2016). The MRI Centre is supported through an NSERC Major Resources Support award. H. Han thanks Oleg Petrov for useful suggestions. We also thank B. Malcolm, M. Olive and B. Titus for their help with mechanical work.

References

- [1] M.A. Bernstein, K.F. King, X.J. Zhou, Handbook of MRI Pulse Sequences, Elsevier Academic press, New York, 2004.
- [2] F. Schmitt, M.K. Stehling, R. Turner, Echo-Planar Imaging, Springer-Verlag, Berlin, 1998.
- [3] W. Block, J. Pauly, A. Kerr, D. Nishimura, Consistent fat suppression with compensated spectral-spatial pulses, Magn. Reson. Med. 38 (1997) 198–206.
- [4] J.C. Haselgrove, J.R. Moore, Correction for distortion of echo-planar images used to calculate the apparent diffusion coefficient, Magn. Reson. Med. 39 (1997) 960–964.
- [5] A. Lingamneni, P.A. Hardy, K.A. Powell, N.J. Pelc, R.D. White, Validation of cine phase-contrast MR imaging for motion analysis, J. Magn. Reson. Imaging 5 (1995) 331–338.
- [6] G. Mason, T. Harshbarger, H. Hetherington, Y. Zhang, G. Pohost, D. Twieg, A method to measure arbitrary k -space trajectories for rapid MR imaging, Magn. Reson. Med. 38 (1997) 492–496.
- [7] Y.T. Zhang, H.P. Hetherington, E.M. Stokely, G.M. Mason, D.B. Twieg, A novel k -space trajectory measurement technique, Magn. Reson. Med. 39 (1998) 999–1004.

- [8] J.H. Duyn, Y.H. Yang, J.A. Frank, Simple correction method of k -space trajectory deviations in MRI, *J. Magn. Reson.* 132 (1998) 150–153.
- [9] D.H. Kim, D.M. Spielman, Reducing gradient imperfections for spiral magnetic resonance spectroscopic imaging, *Magn. Reson. Med.* 56 (2006) 198–203.
- [10] P. Latta, M.L. Gruwel, V. Volotovskyy, M.H. Weber, B. Tomanek, Simple phase method for measurement of magnetic field gradient waveforms, *Magn. Reson. Imaging* 25 (2007) 1272–1276.
- [11] V. Jellus, J.C. Sharp, B. Tomanek, P. Latta, An NMR technique for measurement of magnetic field gradient waveforms, *J. Magn. Reson.* 162 (2003) 189–197.
- [12] A. Takahashi, T. Peters, Compensation of multi-dimensional selective excitation pulses using measured k -space trajectories, *Magn. Reson. Med.* 34 (1995) 446–456.
- [13] M.T. Alley, G.H. Glover, N.J. Pelc, Gradient characterization using a Fourier-transform technique, *Magn. Reson. Med.* 39 (1998) 581–587.
- [14] N. Papadakis, A.A. Wilkinson, T.A. Carpenter, L.D. Hall, A general method for measurement of the time integral of variant magnetic field gradients: application to 2D spiral imaging, *Magn. Reson. Imaging* 15 (1997) 567–578.
- [15] N. De Zanche, C. Barmet, J.A. Nordmeyer-Massner, K.P. Pruessmann, NMR probes for measuring magnetic fields and field dynamics in MR systems, *Magn. Reson. Med.* 60 (2008) 176–186.
- [16] C. Barmet, N. De Zanche, K.P. Pruessmann, Spatiotemporal magnetic field monitoring for MR, *Magn. Reson. Med.* 60 (2008) 187–197.
- [17] D.J. Goodyear, M. Shea, S.D. Beyea, N.J. Shah, B.J. Balcom, Single point measurements of magnetic field gradient waveform, *J. Magn. Reson.* 163 (2003) 1–7.
- [18] D.I. Hoult, R.E. Richards, The signal-to-noise ratio of the nuclear magnetic resonance experiment, *J. Magn. Reson.* 24 (1976) 71–85.
- [19] D.I. Hoult, The principle of reciprocity in signal strength calculations – a mathematical guide, *Concepts Magn. Reson.* 12 (2000) 173–187.
- [20] J. Mispelter, M. Lupu, A. Briquet, NMR probeheads for biophysical and biomedical experiments theoretical principles & practical guidelines, Imperial College press, London, 2006.
- [21] T.L. Peck, R.L. Magin, P.C. Lauterbur, Design and analysis of microcoils for NMR microscopy, *J. Magn. Reson.* 34 (1979) 425–433.
- [22] M. Halse, D.J. Goodyear, B. MacMillan, P. Szomolanyi, D. Matheson, B.J. Balcom, Centric scan SPRITE magnetic resonance imaging, *J. Magn. Reson.* 165 (2003) 219–229.
- [23] P. Jezzard, A.S. Barnett, C. Pierpaoli, Characterization of and correction for eddy current artifacts in echo planar diffusion imaging, *Magn. Reson. Med.* 39 (1998) 801–812.
- [24] T.G. Reese, O. Heid, R.M. Weisskoff, V.J. Wedeen, Reduction of eddy-current-induced distortion in diffusion MRI using a twice-refocused spin echo, *Magn. Reson. Med.* 49 (2003) 177–182.
- [25] M. Alecci, P. Jezzard, Characterization and reduction of gradient-induced eddy currents in the RF shield of a TEM resonator, *Magn. Reson. Med.* 48 (2002) 404–407.